



All-optical generation of coherent in-plane charge oscillations in GaAs quantum wells

Shekhar Priyadarshi,^{1,*} Klaus Pierz,¹ Uwe Siegner,¹ Philip Dawson,² and Mark Bieler¹

¹Physikalisch-Technische Bundesanstalt, Bundesallee 100, D-38116 Braunschweig, Germany

²School of Physics and Astronomy, Photon Science Institute, University of Manchester, Manchester, M139PL, England

(Received 26 January 2011; published 21 March 2011)

We have induced ultrafast charge oscillations in the plane of an unbiased and undoped (110)-oriented GaAs quantum well by coherent optical excitation of heavy-hole and light-hole exciton transitions. The oscillations arise from an in-plane charge displacement between heavy-hole and light-hole states, which results from the periodic parts of the Bloch wave functions and the (110) orientation. The observations are evidence for the existence of a substantial far-infrared transition-dipole moment between heavy- and light-hole subbands for in-plane wave vectors, which we estimate to be $\sim 0.5 e\text{\AA}$ for the quantum well under study. Our findings might prove important for designs of far-infrared detectors and emitters.

DOI: [10.1103/PhysRevB.83.121307](https://doi.org/10.1103/PhysRevB.83.121307)

PACS number(s): 78.67.-n, 72.40.+w, 73.21.Fg

Excitation of semiconductors with ultrashort optical pulses leads to a polarization that coherently couples to the electric field of the excitation pulse. This coherent excitation is responsible for the initial, ultrafast nonlinear response of optically excited semiconductors and has been studied in great detail for both free-carrier and exciton excitations for two decades.¹ One of the fascinating phenomena linked to this coherent regime is the occurrence of quantum beats and the accompanying charge oscillations, the study of which has provided fundamental insight into ultrafast light-matter interactions.²⁻⁵

Quantum beats occur in a three-level system in which two excited states are coupled via a common ground state.^{2,3,6-8} If a transition-dipole moment exists between the two excited states, the quantum beats will be accompanied by charge oscillations with a frequency corresponding to the energy difference between the two excited levels.^{4,5,9,10} Thus, in semiconductor heterostructures, a measurement of the simultaneously emitted electromagnetic radiation, whose frequency is usually within the THz range, is direct evidence of an intersubband transition-dipole moment which cannot be studied by all-optical techniques such as four-wave mixing and transmission measurements.^{4,6} So far, charge oscillations have been measured in a coupled double or in a single asymmetric quantum well (QW) employing beating between two electron subbands^{5,9} and in a single QW employing beating between heavy- and light-hole subbands.⁴ Specifically, the charge oscillations studied in Refs. 4, 5, and 9 resulted from a displacement of the slowly varying envelope function along the growth direction of the QW.

In this paper we report the observation of charge oscillations between heavy- and light-hole exciton states occurring in the plane of an undoped GaAs QW. We take advantage of the (110) orientation of the QW, in which optically excited heavy- and light-hole states lead to oppositely oriented, macroscopic polarizations in the plane of the QW.^{11,12} This in-plane charge displacement results from the periodic parts of the Bloch wave functions and, thus, is of a different physical nature than the one linked to previously observed out-of-plane oscillations.^{4,5,9} Our observations prove the existence of a substantial transition-dipole moment between heavy-hole excitons (HHX) and light-hole excitons (LHX) for in-plane wave vectors in undoped GaAs QWs, which we estimate to be

$0.5 e\text{\AA}$. This study might have consequences for designs of THz emitters and detectors,¹³⁻¹⁵ because, so far, a transition-dipole moment between heavy- and light-hole bands at in-plane wave vectors has only been observed for *p*-type structures where band mixing relaxes the intersubband selection rules.^{16,17} For completeness we would like to emphasize that the observed in-plane charge oscillations are very different from previously observed alternating charge currents induced via quantum interference between ω and 2ω absorption pathways^{18,19} and plasma oscillations.²⁰

In our experiments the in-plane charge oscillations have been triggered by all-optical generation of shift currents^{12,21} in undoped GaAs QWs. Shift currents arise from a shift of the center of the electron charge during excitation and have so far been investigated in a variety of samples.²² For the study described in this paper we employed samples consisting of 40 periods of GaAs wells separated by 8-nm-thick $\text{Al}_{0.3}\text{Ga}_{0.7}\text{As}$ barriers grown on a (110)-oriented GaAs substrate with a 500-nm-thick buffer layer. We studied different samples with well widths of 15, 16, 18, 20, 24, and 28 nm. The samples were excited with laser pulses obtained from a Ti:sapphire oscillator (150 fs, 76 MHz). The peak intensity of the laser pulses could be varied between 10 and 100 MW/cm², resulting in approximate peak carrier densities in the QWs of $3 \times 10^{10} \text{ cm}^{-2}$ and $3 \times 10^{11} \text{ cm}^{-2}$, respectively. The time-dependent shift currents, which are excited by the ultrafast laser excitation, lead to the emission of THz radiation whose time dependence was detected in a conventional free-space THz setup in transmission geometry¹² [see inset of Fig. 1(b)]. Due to the detection geometry being normal to the QW plane, our experiment is only sensitive to currents flowing in the plane of the QW samples. The distinction between currents flowing in different directions in the sample plane was possible with the help of a THz polarizer and a polarization-dependent electro-optic detection crystal.¹² All experiments have been performed at 80 K, except as explicitly mentioned below.

Before addressing the experimental results, we first comment on the symmetry properties of our samples in more detail. In the following discussion we take the *x*, *y*, and *z* directions of our (110)-oriented sample to be parallel to the [001], $[1\bar{1}0]$, and [110] directions, respectively. The QW region of our samples possesses a C_s point-group symmetry²³ having 14 shift current tensor elements: σ_{xxx} , σ_{xyy} , σ_{xzz} ,

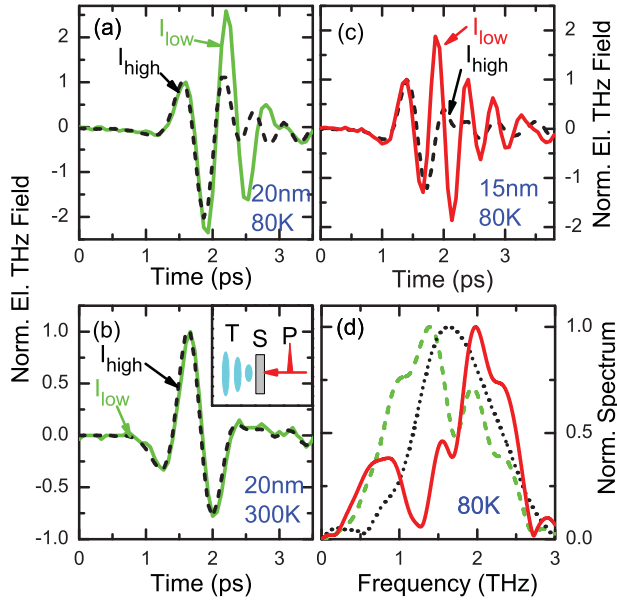


FIG. 1. (Color online) Normalized THz traces obtained from simultaneous excitation of HHX and LHX transitions in a 20-nm QW at 80 K (a), 20-nm QW at 300 K (b), and 15-nm QW at 80 K (c) for high- and low-excitation intensities (dashed and solid lines, respectively). (d) Normalized THz spectra, temperature 80 K: 15-nm QW and high-excitation intensity (dashed green curve is similar to 20-nm QW and high-excitation intensity), 20-nm QW and low-excitation intensity (dotted black), 15-nm QW and low intensity (solid red). The inset of (b) shows a scheme of the setup with the excitation (P: optical pulse) and detection (T: THz radiation) being normal to the sample plane (S).

$\sigma_{xxz} = \sigma_{zxx}$, $\sigma_{xyy} = \sigma_{yyx}$, $\sigma_{yyz} = \sigma_{zyy}$, $\sigma_{zxx} = \sigma_{zxx}$, $\sigma_{zxx} = \sigma_{zxx}$, σ_{zxy} , and σ_{zzz} . Here σ is the third-rank shift current tensor. While the first letter of the subscript denotes the direction of current flow, the other two letters denote the polarization directions of the electric-field components of the excitation pulse. The experiments discussed in this paper take advantage of the σ_{xxx} shift current tensor element for two reasons: (i) The tensor element is absent in the bulk substrate having T_d point-group symmetry. Thus the measured THz traces can be attributed to currents resulting from the QW region only. (ii) Previous experiments¹² have shown that excitation of HHX and LHX lead to oppositely oriented currents. This, in turn, proves that the wave functions of heavy- and light-hole carriers are spatially separated in the plane of the QWs, which is a prerequisite for the observation of in-plane charge oscillations. Recalling that the wave function for the subband state (n) in the QW is given by $\psi_{n,\mathbf{k}_\parallel}(\mathbf{r}) = e^{i\mathbf{k}_\parallel \cdot \mathbf{r}_\parallel} f_{n,\mathbf{k}_\parallel}(z) u_n(\mathbf{r})$ [\mathbf{r}_\parallel and \mathbf{k}_\parallel are the in-plane coordinate and wave vector, respectively, and $f_{n,\mathbf{k}_\parallel}(z)$ and $u_n(\mathbf{r})$ are the slowly varying envelope function and the periodic part of the Bloch function, respectively], it becomes obvious that an in-plane displacement has to stem from the periodic part $u_n(\mathbf{r})$ of the Bloch functions. A possible explanation for this charge displacement, not taking into account the charge oscillations, has been given in Refs. 11 and 24 and is based on permanent dipole moments along the bonds in the GaAs lattice.

We now describe the results of our THz measurements. In Fig. 1(a) are shown two THz traces resulting from σ_{xxx} shift

currents in the 20-nm QW sample after simultaneous excitation of the $n = 1$ HHX and LHX with high (100 MW/cm²) and low (10 MW/cm²) optical peak intensities. While the shape of the high-intensity trace resembles the shape of a typical THz trace measured in our electro-optic detection setup,^{12,25} the low-intensity trace shows significant oscillations immediately after the main pulse. This feature is absent in room-temperature measurements for the same excitation conditions [see Fig. 1(b)]. Thus, we conclude that the oscillation pattern results from a coherent effect which becomes visible due to longer coherence times at low temperatures. Repeating the experiment with a 15-nm QW sample, we again observe oscillations after the main THz pulse, yet this time with a shorter period [see Fig. 1(c)]. A Fourier transformation of the time-domain traces shows that the oscillations shift the peak of the usually obtained THz spectra (green dashed line) to larger frequencies for the 20-nm (black dotted line) and 15-nm (red solid line) QW samples [see Fig. 1(d)]. Moreover, the frequency-domain data suggests that the beat frequencies can be easily retrieved from an analysis of the spectral peaks.

Before performing a more thorough analysis of the beat frequency, we present further evidence that the observed charge oscillations result from a heavy-hole/light-hole beating. In Fig. 2(a) are shown several THz traces obtained from excitation of the 15-nm QW sample with low-excitation intensity for different excitation photon energies. The total THz signal can be considered as a combination of a signal caused by the shift current and a signal caused by charge oscillations. As shown in Fig. 1(d), in the 15-nm QW the two signal contributions have a spectral peak at ~ 1.4 and 2 THz, respectively. Thus, in order to estimate the strength of the beat signal, we performed a Fourier transformation of the time-domain traces and plot the amplitude of the 2-THz frequency component versus excitation photon energy

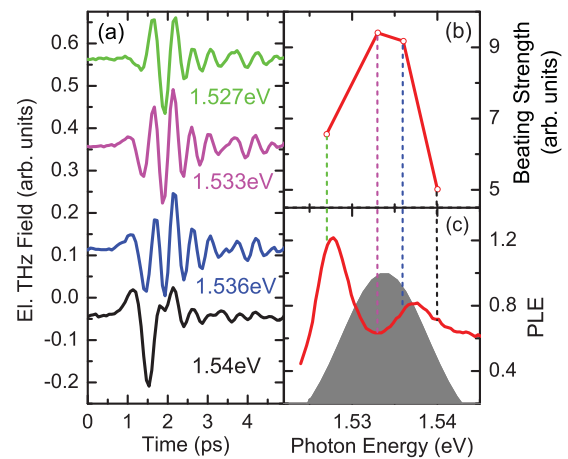


FIG. 2. (Color online) (a) Time-domain THz traces obtained from excitation of the 15-nm QW sample at 80 K for different photon excitation energies. The curves have been shifted along the y axis for clarity. (b) Strength of the spectral components at 2 THz of the THz traces plotted in (a), which has been identified as the beating signal, vs excitation photon energy. (c) PLE spectrum of the 15-nm QW sample showing the $n = 1$ HHX and $n = 1$ LHX transitions. The gray background indicates the spectrum of the excitation laser pulses.

[see Fig. 2(b)]. From a comparison of this curve with the result of a photoluminescence excitation spectroscopy (PLE) measurement plotted in Fig. 2(c) (this measurement shows the photon energies of the $n = 1$ HHX and LHX transitions), it becomes evident that the maximum strength for the beat frequency signal is obtained for simultaneous excitation of the $n = 1$ HHX and LHX transitions. The spectral width of the laser pulses is indicated by the gray background in Fig. 2(c). The results plotted in Fig. 2 confirm that the observed oscillations are triggered by simultaneous coherent excitation of HHX and LHX, yet they also show that the oscillations vanish for continuum excitation, most likely because (i) the intersubband dephasing time between heavy- and light-hole continuum states is considerably shorter than the one for excitons, and (ii) the transition-dipole moment between heavy- and light-hole continuum states with a small wave vector is weaker than for excitons, which are made up of a superposition of continuum states, including states with larger wave vectors.

The exact frequency of the charge oscillations has been extracted by dividing the spectrum of the THz traces measured for low-intensity excitation by the spectrum of the THz traces measured for high-intensity excitation. With this approach we treat the high-intensity THz traces as an impulse response of the whole detection system. The beat frequencies obtained in this manner are plotted in Fig. 3(a) along with heavy-hole/light-hole separation derived from photoluminescence spectra for the various QW samples. As can be seen from Fig. 3(a), there is excellent agreement between the beat frequencies and the heavy-hole/light-hole splitting, which again proves that the measured oscillatory signal arises from charge oscillations between heavy- and light-hole states in the plane of the QW.

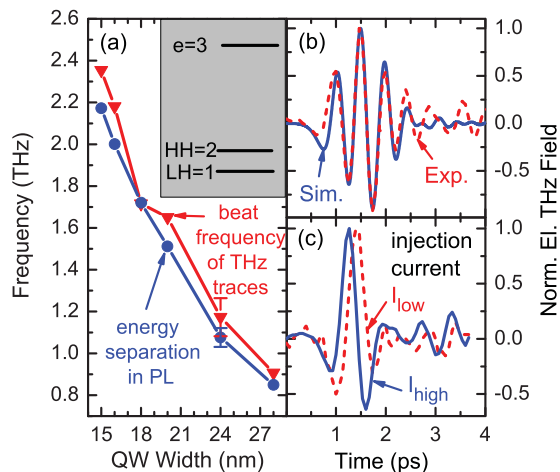


FIG. 3. (Color online) (a) Beating frequency retrieved from THz experiments (red triangles) and energy separation between the $n = 1$ HHX and LHX obtained from PL experiments (blue circles) vs QW width. Inset: Three-level system used for the simulations, including electron (e), heavy-hole (HH), and light-hole (LH) levels. (b) Calculated THz trace obtained from a simple model based on the optical Bloch equations of a three-level system (blue solid line) and the corresponding experimental curve obtained from the 15-nm QW sample (red dashed line). (c) THz traces emitted from injection currents excited along the y direction in the 15-nm QW sample for high- and low-excitation intensities.

In order to quantitatively estimate the transition-dipole moment between HHX and LHX and the corresponding intersubband dephasing time, we numerically solved the optical Bloch equations without the rotating-wave approximation and without considering Coulomb interactions for a three-level system with the energy separations corresponding to the 15-nm QW [see the inset in Fig. 3(a) for the notation of levels]. The resulting macroscopic polarization has been calculated from $P(t) = \mu_{11}\rho_{11}(t) + \mu_{22}\rho_{22}(t) + 2\text{Re}\{\mu_{12}\rho_{12}(t)\}$.¹¹ Here, μ_{11} and μ_{22} are the self-dipole moments⁴ of light and heavy holes, respectively, expressing the shift of charge in the plane of the QW during excitation, and μ_{12} is the transition-dipole moment between heavy and light holes. The density matrix elements are denoted by ρ_{ij} . In the calculation the self-dipole moment of electrons is neglected.²⁴ Moreover, the self-dipole moment of light holes, μ_{11} , is considered to be oppositely oriented¹¹ and three times larger than the self-dipole moment of heavy holes, μ_{22} . The latter assumption is derived from experimental results.¹² The calculated polarization $P(t)$ is double differentiated and filtered with a transfer function denoting the electro-optic detection.²² In the calculations we have varied the dephasing time between heavy and light holes (τ_{12}) and the corresponding transition-dipole moment (μ_{12}). While τ_{12} determines the decay of the oscillatory signal, μ_{12} determines the amplitude of the oscillatory signal with respect to the initial THz signal resulting from the shift of the carriers (μ_{11} and μ_{22}). We obtain the best agreement between experiment and model as illustrated in Fig. 3(b) for $\tau_{12} = 400$ fs and $\mu_{12} = -\mu_{22}/4$. By assuming a self-dipole moment for heavy holes of $2 e\text{\AA}$,²¹ this leads to a transition-dipole moment $\mu_{12} \approx 0.5 e\text{\AA}$ for the 15-nm QW and an excitation photon energy of 1.533 eV.

Such an intersubband transition-dipole moment has only been observed in p -type QWs, where band mixing relaxes the selection rules.^{16,17} We believe that it is the significant band mixing in our (110)-oriented structures²⁶ that leads to a relatively strong transition-dipole moment between HHX and LHX for in-plane wave vectors along the [001] direction.

The study of optically induced currents and their dynamic response is currently receiving a great deal of attention. Recently, a microscopic theory of injection currents launched by all-optical excitation of (110)-oriented GaAs QWs with circularly polarized light has been developed.²⁷ Injection currents result from an optically induced polar carrier distribution in momentum space which, in turn, arises from spin splitting of the subbands. As predicted in Ref. 27, charge oscillations may also occur along the $y = [1\bar{1}0]$ direction if the structure is excited with circularly (or even linearly) polarized light. Yet, for the experimental conditions, in particular the temperature, discussed in this paper, we could not observe any charge oscillations along the y direction, as shown by the THz traces plotted in Fig. 3(c). Thus, even if they exist, the charge oscillations (along the y direction) predicted in Ref. 27 will be weaker than the charge oscillations (along the x direction) observed in our work. Consequently, we conclude that the spatial displacement of the wave functions, which is at the origin of our observations and not included in the theory presented in Ref. 27, is an important prerequisite for the observation of strong charge oscillations. This calls for a more

unified microscopic theory that includes the shift of the center of charges during optical excitation.

In conclusion, we have observed charge oscillations between heavy- and light-hole subbands in the plane of a (110)-oriented GaAs QW sample. In contrast to previous measurements, the charge oscillations do not arise from a displacement of the slowly varying envelope functions of heavy and light holes, but of the periodic part of the Bloch functions. Our observations demonstrate the existence of a strong transition-dipole moment ($\sim 0.5 e \text{ \AA}$) between these subbands for in-plane wave vectors. This might have important consequences for designs of far-infrared lasers and detectors.

In particular, it will be interesting to see whether an applied in-plane electric field enhances the transition-dipole moment and whether the (110) orientation allows for far-infrared gain measurements at elevated temperatures, which have not been possible so far.²⁸

We thank H. T. Duc and T. Meier for useful discussions and A. M. Racu and H. Marx for technical assistance. Financial support by the Deutsche Forschungsgemeinschaft and the Braunschweig International Graduate School of Metrology is gratefully acknowledged.

*shekhar.priyadarshi@ptb.de

¹J. Shah, *Ultrafast Spectroscopy of Semiconductors and Semiconductor Nanostructures* (Springer, Berlin, 1999).

²E. O. Göbel, K. Leo, T. C. Damen, J. Shah, S. Schmitt-Rink, W. Schäfer, J. F. Müller, and K. Köhler, *Phys. Rev. Lett.* **64**, 1801 (1990).

³K. Leo, J. Shah, E. O. Göbel, T. C. Damen, S. Schmitt-Rink, W. Schäfer, and K. Köhler, *Phys. Rev. Lett.* **66**, 201 (1991).

⁴P. C. M. Planken, M. C. Nuss, I. Brener, K. W. Goossen, M. S. C. Luo, S. L. Chuang, and L. Pfeiffer, *Phys. Rev. Lett.* **69**, 3800 (1992).

⁵H. G. Roskos, M. C. Nuss, J. Shah, K. Leo, D. A. B. Miller, A. M. Fox, S. Schmitt-Rink, and K. Köhler, *Phys. Rev. Lett.* **68**, 2216 (1992).

⁶T. Dekorsy, A. M. T. Kim, G. C. Cho, S. Hunsche, H. J. Bakker, H. Kurz, S. L. Chuang, and K. Köhler, *Phys. Rev. Lett.* **77**, 3045 (1996).

⁷M. Joschko, M. Woerner, T. Elsaesser, E. Binder, T. Kuhn, R. Hey, H. Kostial, and K. Ploog, *Phys. Rev. Lett.* **78**, 737 (1997).

⁸M. Koch, J. Feldmann, G. von Plessen, E. O. Göbel, P. Thomas, and K. Köhler, *Phys. Rev. Lett.* **69**, 3631 (1992).

⁹A. Bonvalet, J. Nagle, V. Berger, A. Migus, J. L. Martin, and M. Joffre, *Phys. Rev. Lett.* **76**, 4392 (1996).

¹⁰R. Huber, B. A. Schmid, Y. R. Shen, D. S. Chemla, and R. A. Kaindl, *Phys. Rev. Lett.* **96**, 017402 (2006).

¹¹J. Khurgin, *J. Opt. Soc. Am. B* **13**, 2129 (1996).

¹²M. Bieler, K. Pierz, U. Siegner, and P. Dawson, *Phys. Rev. B* **76**, 161304(R) (2007).

¹³R. Köhler, A. Tredicucci, F. Beltram, H. E. Beere, E. H. Linfield, A. G. Davies, D. A. Ritchie, R. C. Iotti, and F. Rossi, *Nature (London)* **417**, 156 (2002).

¹⁴B. S. Williams, *Nat. Photon* **1**, 517 (2007).

¹⁵B. F. Levine, S. Gunapala, J. Kuo, S. Pei, and S. Hui, *Appl. Phys. Lett.* **59**, 1864 (1991).

¹⁶B. F. Levine, *J. Appl. Phys.* **74**, R1 (1993).

¹⁷Y.-C. Chang and R. B. James, *Phys. Rev. B* **39**, 12672 (1989).

¹⁸C. Sames, J. M. Ménard, M. Betz, A. L. Smirl, and H. M. van Driel, *Phys. Rev. B* **79**, 045208 (2009).

¹⁹D. H. Marti, M. A. Dupertuis, and B. Deveaud, *Phys. Rev. B* **72**, 075357 (2005).

²⁰W. Sha, A. L. Smirl, and W. F. Tseng, *Phys. Rev. Lett.* **74**, 4273 (1995).

²¹F. Nastos and J. E. Sipe, *Phys. Rev. B* **74**, 035201 (2006).

²²M. Bieler, *IEEE J. Sel. Top. Quantum Electron.* **14**, 458 (2008).

²³S. Priyadarshi, M. Leidinger, K. Pierz, A. Racu, U. Siegner, M. Bieler, and P. Dawson, *Appl. Phys. Lett.* **95**, 151110 (2009).

²⁴J. Khurgin, *J. Opt. Soc. Am. B* **11**, 2492 (1994).

²⁵The small oscillations at a later time result from the velocity mismatch between the phase velocity of the THz radiation and the group velocity of the optical pulses in the electro-optic detection crystal.

²⁶S. Priyadarshi, A. M. Racu, K. Pierz, U. Siegner, M. Bieler, H. T. Duc, J. Förstner, and T. Meier, *Phys. Rev. Lett.* **104**, 217401 (2010).

²⁷H. T. Duc, J. Förstner, and T. Meier, *Phys. Rev. B* **82**, 115316 (2010).

²⁸S. Kumar, C. W. I. Chan, Q. Hu, and J. L. Reno, *Nat. Phys.* **7**, 166 (2011).